11R.1 RAINFALL ESTIMATION FROM C-BAND POLARIMETRIC RADAR IN OKINAWA, JAPAN: COMPARISONS WITH 2D-VIDEO DISDROMETER AND 400 MHZ WIND PROFILER

V. N. Bringi[1], M. Thurai[1], K. Nakagawa[2], G.J. Huang[1], T. Kobayashi[3], A. Adachi[3], H. Hanado[2], and S. Sekizawa[2]

[1]Colorado State University, Fort Collins, Colorado, USA
[2]National Institute for Information and Communications Technology, Japan
[3]Meteorological Research Institute, Japan

1. INTRODUCTION

This paper presents a case study of a Baiu front event that occurred on 8-9 June 2004 in the Okinawa region of Japan. The event lasted over 2 days and produced significant rain amounts of over 300 mm at Naha. It was continuously observed by the C-band dual-polarized radar located in Nago, Okinawa. About 15 km NE from the radar, near Ogimi, is a vertical pointing profiler operating at 443 MHz along with a low profile 2D-video disdrometer. Fig. 1 shows the locations of the COBRA radar, and the wind profiler facility at Ogimi. The long Baiu event which included strong convective rain cells separated by stratiform rain (with and without embedded convection) was an excellent case study for inter comparing rainfall characteristics (D_o and rain rate) from three different sensors with widely differing measurement modalities and sampling volumes.

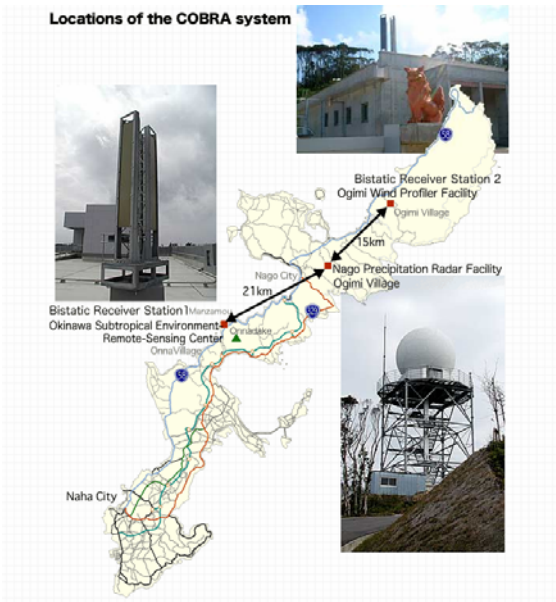

Fig. 1: Locations of the COBRA radar at Nago and the Ogimi wind profiler facility about 15 km to the NE. The 2D-video disdrometer is also located at the wind profiler facility.

*Corresponding author address: V. N. Bringi, Dept. of Electrical Engineering, Colorado State University, Fort Collins, CO 80523-1373, USA.
Email: bringi@engr.colostate.edu

The C-band radar description is given in Nakagawa et al (2003). Table 1 summarizes the radar system parameters. It uses 2 Klystron units, each with a peak power of 250 kW, which can be 'fired' alternately from pulse-to-pulse, or which can be 'fired' simultaneously to synthesize circular or slant linear 45º tilt states. The transmit polarization can be selected from six options, namely, horizontal, vertical, ±45º linear-tilt, right and left hand circular polarizations, all on a pulse-to-pulse basis.

Table 1: C-band COBRA system parameters

Frequency	5340 MHz
Peak power	250 kW (2 Klystron units)
Pulse width	0.5, 1.0 or 2.0 μseconds
PRF	250-3000 Hz, set in steps of 1 Hz
Antenna diameter	4.5 m (parabolic)
Beamwidth	≤ 1.1º
Radome diameter	8 m
Cross-polarisation ratio	≥ 36 dB (beam integrated value)
Antenna gain	≥ 42 dB (including radome)
Sidelobe level	≤ -25 dB (one way)
Antenna scan speed	
PPI	0.5 – 10 rpm (set in steps of 0.1 rpm)
RHI	0.1 – 3.6 rpm (set in steps of 0.1 rpm)
Polarisation (pulse to pulse)	horizontal, vertical, slant linear ±45º tilt, right and left hand circular

In this study the transmitted state was slant linear with tilt of 45°. Two receivers are used to simultaneously measure the signal returns at H and V polarizations from which Z_h, Z_{dr}, Φ_{dp}, and ρ_{co} are obtained. In our study the pulse width was 1.0 microseconds and the range gate spacing was 150 meters. The radar was scanned in PPI mode with PRF of 750 Hz at a rotation rate of 7.8 deg/sec (=1.3 rpm). Data were also collected in RHI mode over the profiler location every 10 minutes throughout the event, the PRF being 1000 Hz and scan rate being 3.0 deg/sec (=0.5 rpm). The number of H or V integration pulses was 32 for the PPI scan and 64 for the RHI scan.

The radar uses a 4.5 m diameter parabolic antenna with a beam width of less than 1.1º. It is covered with an 8 m radome similar to the WSR-88D design and the overall maximum gain is 42 dB including radome effects. Rain on the radome causes attenuation of both reflectivity and Z_{dr}. A number of strong rain cells passed over the radar and during these times we were able to correct the measured reflectivity for rain on radome attenuation using the self-consistency approach to be described later in Section 3 (Gorgucci et al 1999). However, the Z_{dr} was distorted by moderate rain on the radome and these time periods (with R>10 mm/h) are not used in the inter comparisons with the 2D video data.

The 443 MHz wind profiler system at Ogimi is described in T. Adachi et al (2001), see Table 2. There is a 1.3 GHz profiler as well but here we only report on data gathered with the 443 MHz system. The method of retrieving the arbitrarily shaped DSD is based on an iterative procedure developed by Kobayashi and Adachi (2005). The method is dependent on locating the clear-air echo peak which is often masked in strong convective precipitation as occurred during a number of convective rain 'bursts' in the Baiu event.

Table 2: 400MHz-WPR system parameters

Frequency: 443.0 MHz
Power: 20 kW (peak), 2 kW (average)
Pulse width: 1.33, 2.00 or 4.00 μseconds
PRF: 6.25 or 20 kHz
Pulse coding: 1, 4 or 8 bits
First range gate 350 m (minimum)
Antenna size: 10.4X10.4 m (phased array)
Antenna gain: 32.6 dBi
Beamwidth: ≤ 3.3º
Beam steerability: 0 - 360º (azimuth), 0 - 15º

The low profile 2D–video disdrometer manufactured by Joanneum Research was used to measure the DSD with 1 minute averaging. There were 1254 1-min averaged DSDs for the entire event with R>0.5 mm/h. The DSDs were used to estimate the median volume diameter (D_o) and the rain rate (R). The axis ratio of each drop with D>1.5 mm was also measured using the procedure described by Thurai et al (this issue, P11R-15). The mean axis ratio versus D was derived from these data and used for simulating Z_h, Z_{dr} and K_{dp}. The C-band Z_h and Z_{dr} data have to be corrected for rain attenuation. The A_h-K_{dp} and A_{dp}-K_{dp} relations were developed using the measured DSD and mean axis ratio data for the Baiu event. Similarly, the DSD and mean axis ratio data were also used to derive the algorithm to retrieve D_o from Z_{dr} and to retrieve R from K_{dp}. Thus, the attenuation-correction and Do, R retrieval algorithms were based entirely on measurements made with the 2D video instrument during this Baiu event. As such the algorithms are 'tuned' for this event. The applicability of the algorithms to other types of rain events and other climatic regimes needs further validation.

2. OVERVIEW OF 2D-VIDEO MEASUREMENTS

For each 1-min DSD, a normalized gamma model was fitted with the parameters being N_w, Do and μ as described in Bringi et al (2002). Histograms of the Do and $\log_{10}$ (N_w) are given in Fig. 2, the average values being $<D_o>$ = 1.42 mm, $<N_w>$ = 6,000 mm^{-1} m^{-3} (Marshall-Palmer value for exponential shape is 8000), and $<\mu>$ = 5.8.

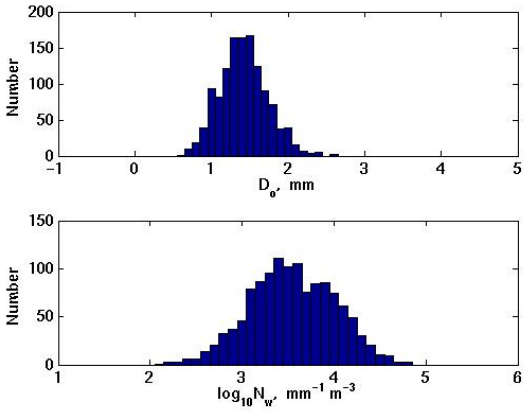

Fig. 2: Histogram of D_o (top panel) and $\log_{10}(N_w)$ from gamma-fitted 1 min DSDs measured by 2D-video disdrometer for the Baiu front event of 8-9 June 2004. Data with R>0.5 mm/h are shown.

Fig. 3 shows D_o and N_w versus R to show the variability of these two DSD parameters with respect to rain rate. Note how the D_o tends to a constant value near 2 mm for R> 50 mm/h from which an equilibrium-type DSD may be inferred. It is obvious that a simple power law between Do and R is not suitable for these DSDs.

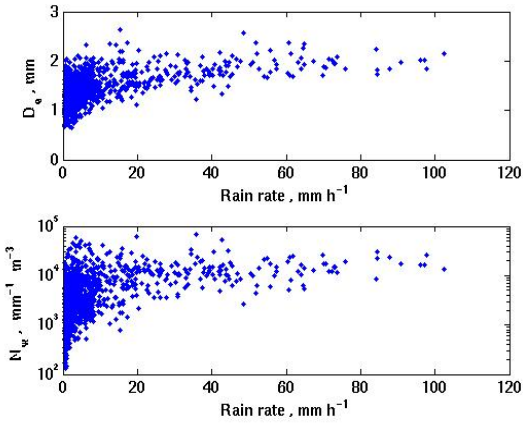

Fig. 3: D_o and N_w versus R from 2D-video data.

Next, we show in Fig. 4 the axis ratio versus D plot and the fit between 1.75-3.75 mm that was used in the simulations of Z_{dr} and K_{dp}. For D<1 mm, the axis ratio is set at 1.0; for 1-1.75 mm and >3.75 mm the static axis ratios of Beard and Chuang (1987) are used. Fig.4 shows color-filled contours of log(number of drops) which fall in a small interval in axis ratio and D akin to a 2D histogram; note that the most probable occurrence or mode is easily seen in the plot on which the best fit mean curve is overlaid:

$$\frac{b}{a} = 1.077 - 0.0964D + 0.0197D^2 - 0.0032D^3 \quad \text{for } 1.75 \le D \le 3.75\,\text{mm} \quad (1)$$

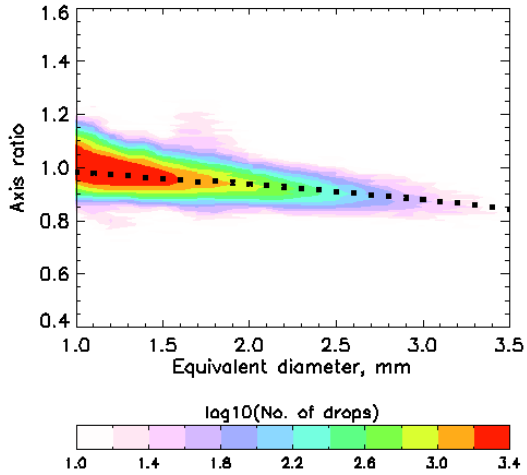

Fig.4: Color-filled contours of log(number of drops) showing the variation of axis ratio versus D from 2D-video disdrometer measurements for the Baiu event. The square marks denote the fit given in (1) for 1.75<D<3.75 mm. For D<1.75 or D>3.75 mm the Beard and Chuang (1987) fit is used.

The above mean fit accounts for a small upward shift in axis ratio due to steady state drop oscillations as measured by the 2D video disdrometer for the Baiu front dataset. The predominant oscillation mode from these data was inferred to be the oblate-prolate mode; see also Thurai and Bringi (2005) and Thurai et al (this issue, P11-R15).

From the normalized gamma-fitted DSD data and the mean axis ratio versus D in Fig. 4, we simulate the radar observables Z_h, Z_{dr} and K_{dp} along with specific attenuation at H-polarization (A_h) and the differential attenuation between H and V polarizations (A_{dp}). The canting angle distribution is assumed to be Gaussian with mean 0 and standard deviation of 5 degrees, to account for turbulence. Fig. 5 shows the plot of D_o versus Z_{dr} (expressed as a ratio below and not in dB) along with the best fit lines:

$$D_o = 3.984\ Z_{dr}^{linear} - 3.2303;\ \text{mm for } Z_{dr}^{linear} \le 1.3 \quad (2a)$$

$$= 0.733\ Z_{dr}^{linear} - 0.9088;\ \text{mm for } Z_{dr}^{linear} > 1.3 \quad (2b)$$

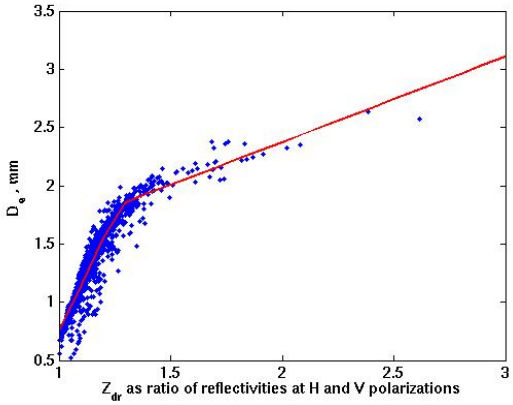

Fig. 5: D_o versus Z_{dr} (as ratio) from 2D-video data along with best fit lines used in the retrieval algorithm.

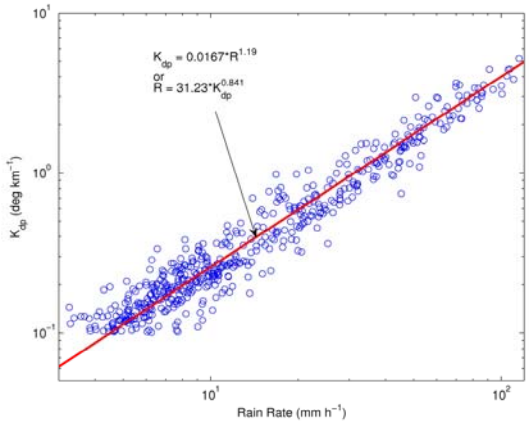

Fig. 6: As in Fig. 5 except K_{dp} versus R along with best fit power law used in the retrieval algorithm.

The best fit lines are used to retrieve D_o from radar measured Z_{dr} (shown later in Section 4). Fig. 6 shows the plot of R versus K_{dp} (both in logarithmic scale) and the best fit power law $R=31.2\ K_{dp}^{0.84}$ which is used later to retrieve R from radar measurements of K_{dp}. The R-K_{dp} relation derived here is similar to that derived using Joss disdrometer data from Darwin, Australia as described in Bringi et al (2001), $R=32.4K_{dp}^{0.83}$. Finally, we give the best fit power laws, (see, also, Thurai et al, this issue, P11R-15) again based on simulations, for A_h vs. K_{dp}, A_{dp} vs. K_{dp} and K_{dp}/Z_h vs. Z_{dr} as follows:

$$A_h = 0.05623 K_{dp};\ \text{dB/km} \quad (3a)$$

$$A_{dp} = 0.00736 K_{dp}^{1.133};\ \text{dB/km} \quad (3b)$$

$$\frac{K_{dp}}{Z_h^{linear}} = 4\ 10^{-5}\left(Z_{dr}^{-0.447}\right);\ \text{deg/km per mm}^6\ \text{m}^{-3} \quad (4)$$

The first two fits are used for attenuation-correction procedures for Z_h and Z_{dr} to be described later. The third fit is used for the self-consistency procedure for fine tuning of the system radar constant using the rain medium whereby Z_h and Z_{dr} (after attenuation correction) are used to predict K_{dp} and hence to predict range profiles of Φ_{dp} which is compared against the measured Φ_{dp} . Examples will be shown in the next section.

3. OVERVIEW OF RADAR MEASUREMENTS AND ATTENUATION CORRECTION

The Baiu front episode of 8-9 June, 2004 lasted for more than 20 hours with many convective bursts followed by stratiform rain with bright-band and with embedded convection. We have selected three periods for analyses, viz, (a) 03:00-0700, (b) 11:00-15:00 and (c) 15:00-19:00 UTC (8 June 2004). Because the Z_{dr} is based on signals received via 2 receivers (termed as H and V receivers) any systematic gain offset between the two receivers must be established. Receiver calibration data from the two receivers also showed that the gain difference was dependent on the input signal level which proved to be a complicating factor in the Z_{dr} calibration. Since two transmitters are involved in synthesizing the radiated polarization, any small difference in the transmitted powers must be known and corrected for.

After Z_{dr} calibration, the measured Z_h and Z_{dr} data were corrected for rain attenuation using an adaptation of the method described in Tan et al (1995) and using the power law coefficients given above in (3). The method utilizes the range profile of K_{dp} derived using the iterative filtering method of Hubbert and Bringi (1995). The correction is done gate-by-gate, for both Z_h and Z_{dr} as illustrated in the middle and bottom panels of Fig. 7.

To ensure self-consistency, the corrected Z_h and Z_{dr} are used to reconstruct the Φ_{dp} profile using (3) and compared with the measured profile, as illustrated in the top panel of Fig. 7. A 2 dB adjustment to the nominal COBRA radar constant was sufficient for the predicted Φ_{dp} to closely 'track' the measured Φ_{dp}. Note this method has been demonstrated at S-band previously (Goddard et al 1994); however, the example given in Fig 7 (top panel) shows that the self-consistency method can be used for C-band also, where rain attenuation affects both measured Z_h and Z_{dr}. Unlike Tan et al's method which used the coefficients derived for Marshall-Palmer DSD, in our method the power law coefficients in (3) are based on the drop axis ratios and size distributions measured by the 2D-video for this intense Baiu event. The PPI of the attenuation-corrected Zh is shown in Fig 8. The range profile of Fig. 7 is along the 45 degree azimuth corresponding to the convective line of Fig. 8.

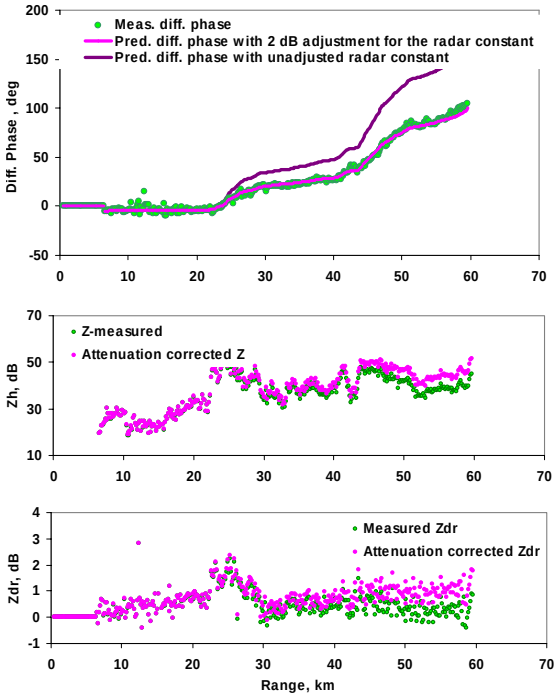

Fig. 7: (Top panel) Example range profile showing self-consistency principle to adjust the nominal radar constant (in this case a 2 dB reduction was indicated), middle panel shows attenuation-correction for Z_h while lower panel shows same for Z_{dr}.

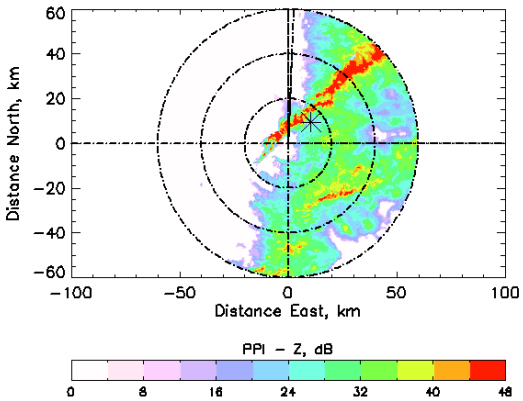

Fig. 8: PPI scan data at 1.5 degree elevation angle of the attenuation-corrected Z_h showing a 'snap shot' of the Baiu front event at 13:43 UTC on 8 June 2004. The 'star' marks the location of the Wind Profiler and 2D-video instrument about 15 km along the 45 degree azimuth angle.

By applying the self consistency method to the full PPI dataset, it was possible to adjust the radar constant accurately using the histogram of the difference between the predicted and the measured Φ_{dp} at the 60 km range. This was more representative than using single selected beams. The histogram corresponding to the PPI scan is given in Fig. 9. The

radar constant was adjusted until the mean of the histogram became zero. This method also enabled estimation of additional attenuation introduced by rain on radome. A rain gauge at the radar site confirmed that that extra attenuation could be correlated/tracked with the rain rate (see Fig. 10).

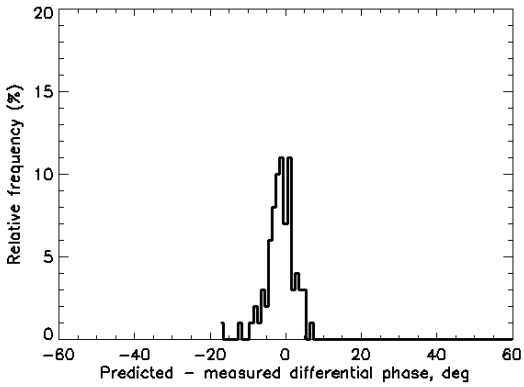

Fig. 9: Histogram of the difference between predicted Φ_{dp} and measured Φ_{dp} at 60 km range for the entire PPI scan shown in Fig. 8 after applying the 2 dB adjustment to the radar constant.

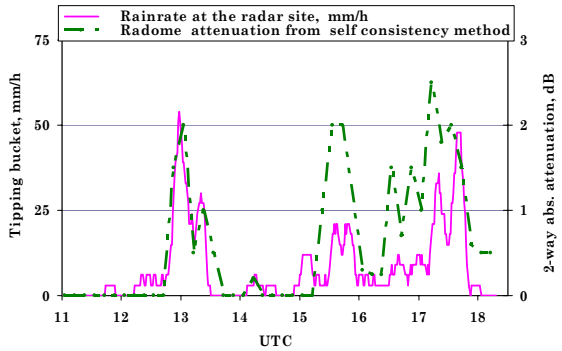

Fig. 10: Excess attenuation due to rain on radome estimated using the self-consistency principle (pink curve). Green dashed trace is from rain guage at the radar site.

For completeness, we show in Fig. 11 the intensity plots of attenuation-corrected Z_{dr} versus Z_h, and K_{dp} versus Z_h (similar to the intensity plot shown in Fig 4 except on a log(relative frequency) color scale). Data from the full PPI scan in Fig. 8 are used for this plot. Overlaid on these plots are the expected trends (mean±1σ) based solely on simulations of the radar parameters using the measured 2D-video DSDs and the axis ratios of Fig. 4. The close agreement between the mode of the radar-derived distributions and the 2D-video based distributions gives added confirmation for the accuracy of the system calibration and the attenuation-correction methodology.

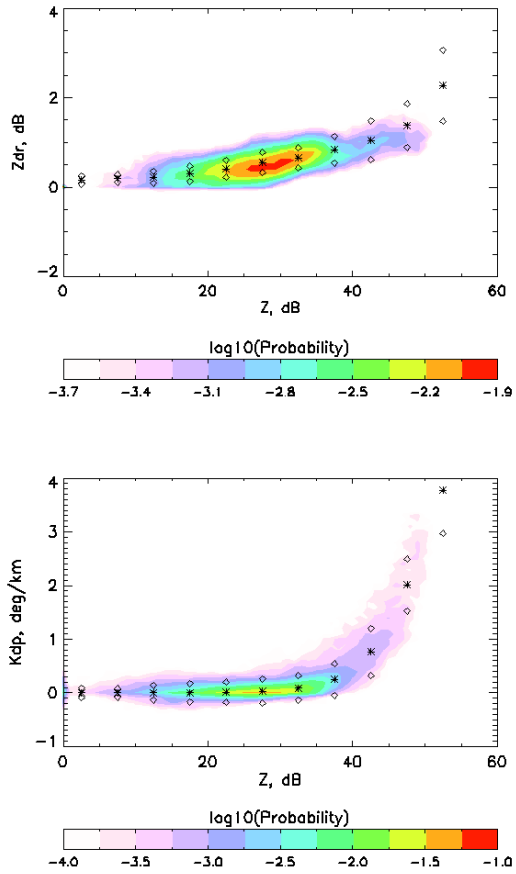

Fig. 11: Color-filled contours of log(relative frequency) showing the variation of Z_{dr} vs. Z_h (top panel) and K_{dp} vs. Z_h (bottom panel). Data from the PPI scan in Fig. 8. The 'star' marks the mean trend from 2D-video based simulations along with ±1σ deviation ('open circle' marks).

4. INTERCOMPARISON OF RESULTS

PPI scans at 1.5 degree elevation angle over the 2D video disdrometer site were available every 10 minutes. RHI scans over the same site were also available every 10 minutes. Radar data from the PPI scans were averaged over a polar area measuring 1 km X 4 deg centered on the 2D video location. For the RHI scans, the data between 200-500 m in height and 1 km in range (centered over the 2D video site) were averaged. In either case data from around 35 range gates were included in the averaging window. The 2D video DSD data were averaged over 1 min and the Z_h, Z_{dr} and K_{dp} were simulated using the axis ratios shown in Fig. 4 (the actual DSD was used in the simulations, not the gamma-fitted versions). The 2D video-based estimates of Z_h, Z_{dr} and K_{dp} were then time-sampled at the time of the radar data. Fig. 12 shows the scatterplots for Z_h, Z_{dr} and K_{dp}.

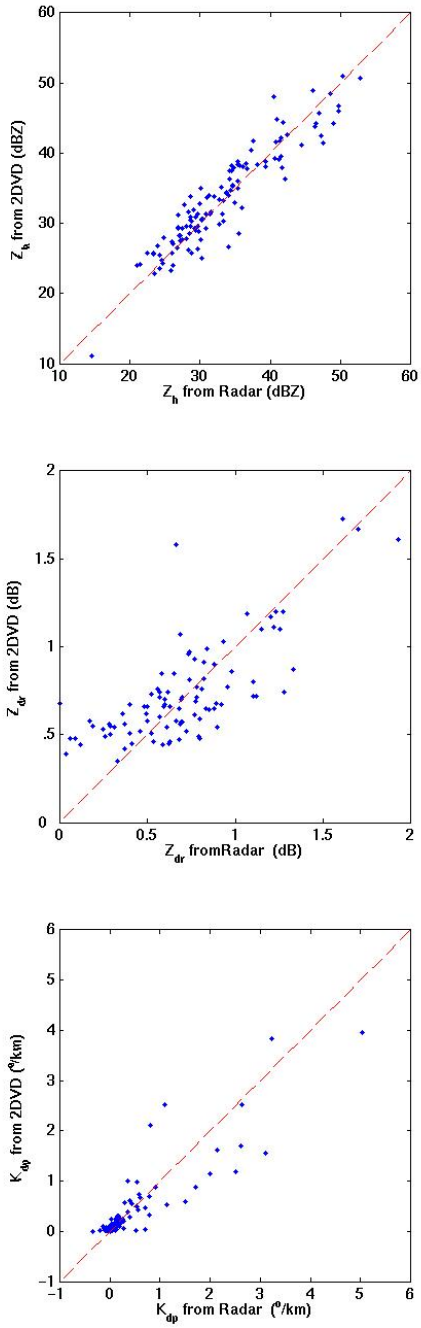

Fig. 12: Scatter plots of 2D-video based simulations of radar parameters versus radar observations averaged over the 2D-video site for the entire Baiu event. Z_{dr} data corresponding to rain on radome > 10 mm/h has been excluded.

For the reflectivity comparisons, the agreement is excellent despite the differences in the sampling volumes and the highly convective nature of this event. The agreement lies within the expected errors of the 2 instruments. For the Z_{dr} case, the scatter is likely to be due to the gain difference between the H and V receivers not being constant through the dynamic range, rather being dependent on the input signal strength. Although attempts were made to correct for the gain mismatch via a mean fit to the receiver calibration data, residual error still remained which may have contributed to the scatter in the Z_{dr} inter comparisons. Radar Z_{dr} data at times during which rain on radome exceeded 10 mm/h were removed because of the distortion which became evident when inspecting the Z_{dr} versus Z_h intensity plot for each of the PPI/RHI scans. Whilst it was possible to compensate the Z_h for the extra rain on radome attenuation as explained earlier, it was not possible to adjust for the Z_{dr} distortion. The K_{dp} inter comparisons are reasonable (and unaffected by rain on radome or rain attenuation) in spite of the smoothing interval required for the radar estimates, especially during the highly convective periods of the Baiu event.

Finally in Fig.13, we make an overall comparison between the 2D-video, Wind Profiler and the COBRA radar retrievals of D_o and R for three time periods (03:00-07:00, 11:00-15:00 and 15:00-19:00 UTC) of the Baiu event. The color image in the top panel represents the 1-min DSD from the 2D-video, in terms of log(number of drops) in each diameter interval of 0.25 mm. The D_o and R from COBRA radar were estimated from Z_{dr} and K_{dp} using the fits shown in Figs. 5 and 6, respectively. For K_{dp}<0.1 deg/km a Z_h-R relation was used for estimating R. This $Z_h=288R^{1.34}$ relation was based on 2D video data for this event and 'tuned' for low rain rates < 4.5 mm/h, in effect being valid for the stratiform portions of the Baiu event.

For the Wind Profiler, the D_o and R were estimated from the N(D) which was estimated, without assuming an apriori form, from the Doppler spectra as described by Kobayashi and Adachi (2005). The method is an iterative retrieval procedure for arbitrary N(D) and gives the vertical profile of derived parameters such as D_o and R. Here we have taken the rain rate retrieval from the 550 m altitude and the Do retrieval from the 700 m altitude as these gave the best inter comparisons with the 2D video data. Since the measured Doppler spectrum is the convolution of the precipitation spectrum and the turbulent clear air spectrum, deconvolution of the Doppler spectrum is achieved through repeated convolutions.

The first period from 03:00-07:00 was largely stratiform in nature except for a 30 min convective period between 05:30 and 06:00. The inter comparison is very good between the 3 instruments for this first period. The D_o estimates lie within a narrow range, mostly in the 1.3-1.8 mm interval, with no clear dependence on rain rate, even in the 20-30 mm/hr convective period. The larger rain rate in this period is due to the larger concentrations of small drops around 1 mm.

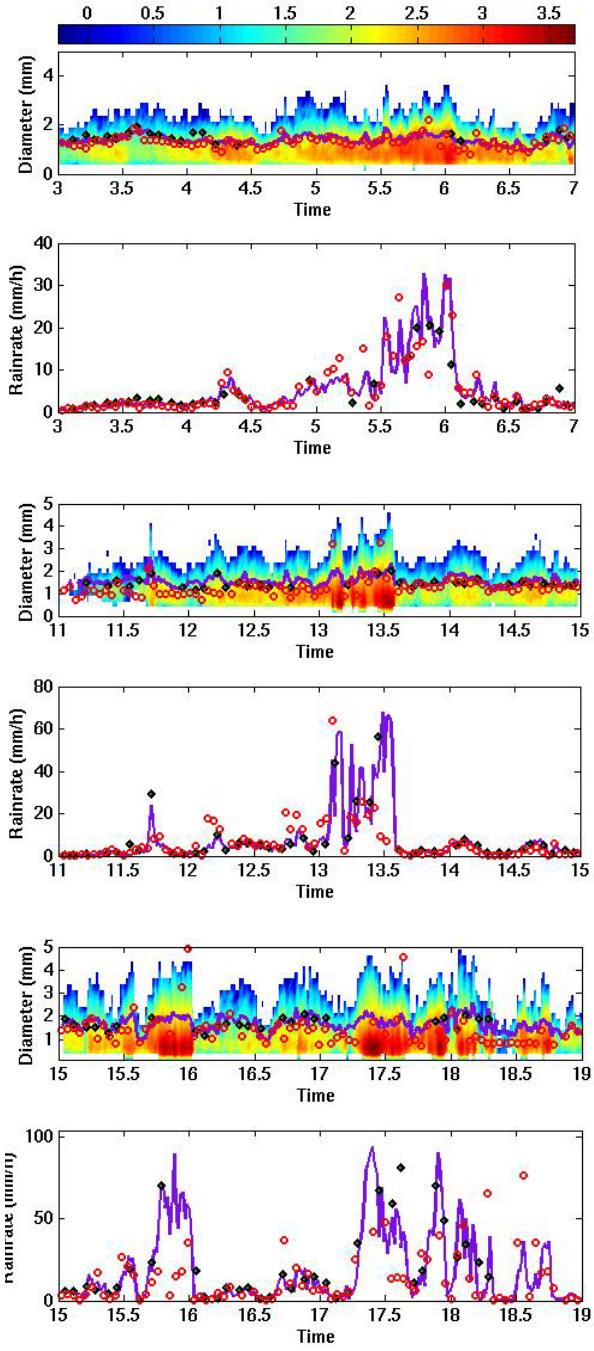

Fig. 13: Comparisons of D_o and R between COBRA radar, Wind Profiler and 2D-video based retrievals for three periods of the Baiu event (horizontal axis is decimal UTC time on 8 June 2004). The color-filled contours show $\log_{10}(N(D))$ from 2D-video at 1 min intervals. Red circles mark the data from Wind Profiler, black diamonds (with green infill) mark data from COBRA radar and purple trace is from 2D-video data. D_o from COBRA is excluded when rain on radome exceeds 10 mm/h.

The second period shows a one convective burst between 13:00 and 13:30 with a noticeable increase in the number of larger drops. Some underestimate with the wind profiler retrievals is seen near 13:30 due to masking of the clear air echo peak by the rain echo in the Doppler spectra. The rain rate was estimated by assuming the clear air peak as a fixed Gaussian function for such cases. In addition, the boundary of the clear air peak and the precipitation peak, that is the minimum position of the two peaks, appeared at a relatively large Doppler velocity. This indicates that the rain rate was calculated from DSD ranging from relatively large diameter and thus leads to the underestimate of R.

The COBRA and wind profiler retrievals are in good agreement with the 2D video for almost the entire second period except for a systematic underestimate in Do from wind profiler during 11:00-12:15. The third period has several convective bursts; overall, the agreement between the three instruments is good considering the strong variability in the rain rate.

The overall comparisons indicate that the three instruments are in good agreement especially during the more steady rain periods. There is more scatter during the convective rain periods as expected. The COBRA radar estimates are accurate through out the three periods except for cases with very small Do's (less than 0.5 - 0.6 mm) which correspond to small Z_{dr} values of less than around 0.3 dB. At such small Z_{dr} values, the use of two somewhat mismatched receivers combined with slant 45 deg linear transmission, small number of integration samples and receiver noise (which has not been corrected for in these data) leads to larger measurement fluctuations. This limits the lower bound of the Do estimates to 0.5-0.6 mm with the scan parameters/configuration used for these observations. Very high accuracy in Z_{dr} measurements at low levels requires (i) pulse-to-pulse H/V switched transmission, (ii) alternate reception with a single receiver, (iii) large dwell times and (iv) accurate correction for the receiver noise.

5. CONCLUSIONS

The data reported here inter compare D_o and rain rates from three different instruments with vastly different sampling volumes, time resolutions, observation strategies and physical bases for the retrievals. The Baiu front event studied here was a prolonged one, with a significant mix of stratiform and convective rain types. The retrieval algorithms used for the C-band radar were wholly based on the dsd and drop axis ratio information derived for this particular event from 2D-video disdrometer as opposed to using a standard dsd/axis ratio models for the retrievals. The attenuation-correction algorithms

for Z_h and Z_{dr} based on K_{dp} also utilized power law coefficients derived from the 2D-video data. The self-consistency method was used to adjust the radar constant even during rain on radome periods. Probability-based scatter plots of Z_{dr} versus Z_h and K_{dp} versus Z_h from the radar PPI/RHI scan data, after attenuation correction and self consistency adjustment, were remarkably close to the 2D-video derived simulations. Further verification was provided by scatter plots of Z_h, Z_{dr} and K_{dp} from radar data spatially averaged over the disdrometer site. Time series comparisons of D_o and rain rate from COBRA radar and the 2D-video showed close agreement within the error bounds of both instruments. When compared further with retrievals from a wind profiler collocated with the 2D-video, good agreement was found during the steady, more stratiform periods of the Baiu event. The wind profiler estimate contains some inaccurate results during the highly convective rain periods which results in relatively large scatter of the data. A quality control procedure to remove such data may be needed to improve the results.

ACKNOWLEDGEMENTS

Three of the authors (VNB, MT and GJH) acknowledge support from the National Science Foundation via grant ATM-0140350. The collaboration between CSU and NICT was made possible by travel funds from NICT to Prof. V.N. Bringi. The authors are grateful to Michael Schoenhuber of Joanneum Research for assistance with processing of the 2D-video disdrometer data.

REFERENCES

Beard, K.V. and C.Chuang, 1987: A new model for the equilibrium shape of raindrops, J. Atmos. Sci., vol. 2, 468-471.

Bringi, V.N., G.J. Huang, V. Chandrasekar and T.D. Keenan, 2001: An areal rainfall estimator using differential propagation phase using a C-band radar and a dense gauge network in the Tropics, J Atmos Ocean Tech, vol. 18, 1810-1818.

Bringi, V.N., G.J. Huang, V. Chandrasekar and E. Gorgucci, 2002: A methodology for estimating the parameters of a gamma raindrop size distribution model from polarimetric radar data: Application to a squall line event from the TRMM/Brazil campaign, J Atmos Ocean Tech, vol. 19, 633-645.

Goddard, J.W.F., J. Tan and M. Thurai, 1994: A technique for calibration of meteorological radars using differential phase, IEE Electronics Letters, vol. 30, 166-167.

Gorgucci, E., G. Scarchilli and V. Chandrasekar, 1999: A procedure to calibrate multiparameter weather radar using properties of the rain medium, Trans IEEE, Geosci and Remote Sensing, vol. 17, 269-276.

Adachi. T, Y. Masuda, and S. Fujii, 2001: Development of a 400MHz-band Wind Profiler Radar in Okinawa, The Third International Symposium on Asian Monsoon System (ISAM3), pp. 309-313.

Hubbert, J. and V.N. Bringi, 1995: An iterative filtering technique for the analysis of copolar differential phase and dual frequency radar measurements, J Atmos Ocean Tech, vol. 12, 643-648.

Kobayashi, T. and A. Adachi. 2005: Retrieval of Arbitrarily Shaped Raindrop Size Distributions from Wind Profiler Measurements. J Atmos and Ocean Tech, vol. 22, 433–442.

Nakagawa, K., H. Hanado, S. Satoh, N. Takahashi, T. Iguchi and K. Fukutani, 2003: Development of a new C-band bistatic polarimetric radar and observation of Typhoon events, Proc. 31st Conf Radar Meteor, 6-12 August, AMS, vol. 2, 863-866.

Tan, J., J.W.F. Goddard and M. Thurai, 1995: Applications of differential propagation phase in polarisation-diversity radars at S- and C-band, International Conference on Antennas and Propagation, IEE Conf. Publication Number 407, Eindhoven, NL, April.

Thurai, M. and V.N. Bringi, 2005: Drop Axis Ratios from 2D Video Disdrometer, J Atmos Ocean Tech, vol. 22, 963–975.

Thurai, M., V.N. Bringi, K. Nakagawa, T. Kozu, M. Schönhuber and T. Shimomai, 2005: Drop axis ratio and fall velocity distributions in rain from 2-D video disdrometer, *this issue*, P. 11R-15, 32nd Conf. on Radar Meteor., 24-29 Oct 2005, Albuquerque, NM.